Young-type Interference in Soft Lepton Scattering of Diatomic Homonuclear Molecules

Marcos V. Barp[1] | **Felipe Arretche**[1]

[1]Physics Department, Universidade Federal de Santa Catarina, 88040-900, Florianópolis, Santa Catarina, Brazil

Correspondence
Marcos V. Barp, Physics Department, Universidade Federal de Santa Catarina, 88040-900, Florianópolis, Santa Catarina, Brazil
Email: marcos.barp@posgrad.ufsc.br

Funding information
N/A

Interference patterns in the scattering of positrons and electrons by diatomic homonuclear molecules are *ab initio* calculated. Our results are compared to model potential calculations with incident particles in twisted and plane wave states. All calculations are obtained in the first Born approximation framework. The comparison of the elastic differential cross sections shows how an *ab initio* description of the electronic molecular structure influence the interference minima structure. The origin of such patterns are also discussed.

Keywords — Positron and electrons scattering, Elastic scattering, Interference, high energy.

1 | INTRODUCTION AND MOTIVATION

One of the groundbreaking contributions of Louis de Broglie [1] to modern physics is the concept of wave-particle duality. Such interpretation comes from the inability of the classical definitions *wave* and *particle* to describe entities and its behaviour in quantum scale. This sense, theoretically established in 1923, had impact in the understanding of previous and forthcoming experiments.

In the beginning of the 19th century, Young [2] demonstrated the wave-like behaviour of light observing the interference patterns by a plate with two parallel slits exposed to coherent light, later referred to as *double-slit experiment*. More than a hundred years after that, Davisson and Germer [3] observed similarities when studying the diffraction of electrons by a crystal of nickel, in 1928. These scattered electrons formed patterns of interference analogous to the ones detected by Young, demonstrating the wave-like nature of electrons.

Similar behaviours were also observed by recent investigations with a variety of sources, including photons [4, 5, 6, 7], protons [8], neutrons [9], electrons [10, 11, 12, 13], atoms [14, 15] and ions [16, 17, 18] beams, notably, the electron emission from H_2 by ion impact [19, 20, 21], collisions between hydrogen molecular ions and helium [16],

electron loss in ion-molecule collisions [22, 23], proton-diatomic molecule scattering [24, 25] and photoionization of molecules [26, 27, 28, 29].

In the field of electron and positron scattering, the natural analogous system to Young's experiment is the homonuclear diatomic molecule one [30, 31, 32, 33] due to its symmetry. Akin interference patterns were noticed, for example, in the differential cross sections (DCSs) of molecular nitrogen ionization by electron impact [34], exhibiting structures of minima when the molecule is considered aligned, *i.e.*, the molecules are modeled with a defined macroscopic orientation to the incident beam in the scattering process.

Recently, Maiorova *et al.* [35] conducted an investigation on the Young-type interference patterns in the elastic DCS of molecular hydrogen by electrons. These authors considered an incident twisted electron beam, *i.e.*, if the propagation of the incident beam is said to be in the $\hat{z}$ axis, the electron state can be understood as a coherent superposition of the plane waves, whose wave vectors $\vec{k} = (\vec{k}_\perp, k_z)$ lay on the surface of a cone with the opening angle $\tan \theta_k = \frac{|\vec{k}_\perp|}{k_z}$, as stated in Karlovets *et al.* [36]. The DCSs were computed with the independent atom model (IAM) [37, 38], which considers noninteracting atoms to construct the molecule, in the first Born approximation (FBA) framework for 100 eV and 1 keV energies. In order to apply the IAM, these authors have assumed the electron-atom interaction to be the superposition of two Yukawa potentials, that approximate the Coulomb field of the nucleus, screened by the target electrons. The interference patterns were reported for the perpendicular and parallel orientation of the molecule to the incident beam.

The FBA has been used as a valuable tool to investigate intermediate and high energy elastic electron scattering by molecules since the first investigations on the theme [39]. Working in the context of FBA, Inokuti and McDowell [40] built a theory that allows direct correlations between zero angle scattering (low transferred momentum) and expected values from the charge density of the atomic target. Applying a molecular version of this theory, Liu [41] presented a series of results on electron-H_2 and N_2 scattering using molecular wavefunctions with a high degree of precision. Roughly speaking, the theory applied by Liu, like the original theory of Inokuti and McDowell, is constructed from an expansion for very small transferred momentum (small scattering angle) of the Fourier transform of the target's electron density.

One of the main goals of this works is to fulfill the room left by these two works, *i.e.*, to provide an improved FBA calculation valid for any value of the transferred momentum performed and going beyond the IAM formulation. More precisely, we propose an *ab initio* method to compute the elastic scattering of electrons and positrons (from now on "leptons") by diatomic homonuclear molecules. In spite of the fact that an appropriate description of the near zero angle scattering demands the inclusion of exchange and polarization effects [42] we consider only the static interaction at this moment. Therefore, the results obtained are valid to both positron and electron impact. We choose to work with FBA due to the high energy regime we are interested in ($10^2 - 10^3$ eV).

We have considered Gaussian-type orbitals, in order to describe the molecular target, from an unrestricted Hartree-Fock (UHF) approach, giving this model open-shell capabilities. From *ab initio* calculations one expects accurate results not necessarily in agreement with experiment. As well understood in the literature, the IAM approach disregards any chemical bond effect. The *ab initio* molecular wavefunction applied here, compared to the form factor-based models, provides an efficient tool to investigate the influence of the charge density description for high energy scattering. Furthermore, these results based in the fundamental ingredients of the scattering field will be used as benchmark, by our research group, in the development of more sophisticated open-shell scattering methods.

As we will see, the formation of interference patterns in the DCSs is strongly connected to the relative orientation of the molecule to the direction of the incident particle. This "relative orientation" effect determines the respective superposition of nuclear and electronic scattering amplitudes showing remarkable differences for parallel and perpendicular configurations. In the same spirit, simple wave mechanics reasoning allows one to understand the interference

patterns in homonuclear diatomics in general connecting the ratio between the molecular geometry and the de Broglie wavelength of the incident lepton.

This paper is organized as follows: In section 2 we describe the theory developed in order to compute the differential cross sections; Section 3 we show and discuss the results obtained; Section 4 we state our conclusions and final comments. Atomic units (a.u.) are used in this paper unless stated otherwise[1].

2 | THEORY

In the context of positron and electron scattering there is a huge difference in the modeling of atomic and molecular targets. Atoms are essentially central potential systems with electronic structure. Molecules, on the other hand, are characterized by vibrational and rotational states combined to a more complex electronic structure due to the presence of chemical bonds. For scattering calculations, even when the fixed-nuclei is considered and the vibrational and rotational degrees of freedom are disregarded, the major difficulty is found in the non-central nature of the interaction potential [43]. Hence, in the molecular scenario, one must pay attention to the orientation of the target, since it plays a central role in the process. This task is done by the Euler angles [44] ($0 \leq \alpha \leq 2\pi$, $0 \leq \beta \leq \pi$ and $0 \leq \gamma \leq 2\pi$) which describe the orientation of a rigid body as regards to a fixed coordinate system. For diatomic molecules, due to symmetry, these three angles can be reduced to polar (β) and azimuth (α) only.

In our calculation, the usual form of the electrostatic potential in atomic units have been used for M nuclei and N electrons, given in the coordinate representation by:

$$V = q \sum_{A=1}^{M} \frac{\mathcal{Z}_A}{|\vec{x} - \vec{R}_A|} - q \sum_{e=1}^{N} \frac{1}{|\vec{x} - \vec{r}_e|} = V_{nuc} + V_{elec} \, , \tag{1}$$

where q is a dimensionless constant equal to ± 1 for positrons and electrons, upper and lower sign respectively. The spatial location of the incident particle and the molecular electrons are, respectively, $\vec{x}$ and $\vec{r}_e$, and $\vec{R}_A$ is the vector that locates the nuclei. The atomic number of the centers are described by $\mathcal{Z}_A$.

From quantum scattering theory, the scattering amplitude can be separated into nuclear and electronic terms. Considering (1), the scattering amplitude reads:

$$\mathcal{F}(\vec{k}_f, \vec{k}_i) = -\frac{1}{2\pi} \langle S_{\vec{k}_f} | \hat{V}_{nuc} | S_{\vec{k}_i} \rangle - \frac{1}{2\pi} \langle S_{\vec{k}_f} | \hat{V}_{elec} | S_{\vec{k}_i} \rangle = \mathcal{F}_{nuc} + \mathcal{F}_{elec} \, . \tag{2}$$

It is worth noting that $S_{\vec{k}}$ is the homogeneous solution of the corresponding Lippmann-Schwinger equation associated to the Hamiltonian $\hat{H} = \hat{T}_p + \hat{H}_{mol} + \hat{V}$. The kinetic energy operator of the incident particle is denoted by $\hat{T}_p$, $\hat{H}_{mol}$ is the molecular Hamiltonian and $\hat{V}$ is the scattering potential operator.

The representation of the homogeneous solution, already considering the Born-Oppenheimer approximation and the FBA, is given by

$$|S_{\vec{k}}\rangle = |\Phi_0^{nuc}(\vec{R}_A)\rangle \otimes |\phi_0(\vec{s}_N)\rangle \otimes |\vec{k}\rangle \, , \tag{3}$$

where the nuclear wavefunction Φ_0^{nuc} does not contribute to the result due to the fixed nuclei approximation. The

---

[1]In atomic units, reduced Plank's constant $\hbar$, elementary charge e and electron rest mass m_e are equal to one. Also, a few relations are useful to the understanding of this paper regarding atomic units. Wavevector k, wavelength λ and energy E: $k = \frac{1}{\lambda}$, $\lambda = \frac{1}{\sqrt{2E}}$. Where the unit of energy in a.u. is twice the binding energy of hydrogen $1 a.u. = 27.211 eV$.

scattering particle state is described by $|\vec{k}\rangle$ and the electronic wavefunction is represented *via* the Slater determinant for K orbitals and N electrons

$$\phi_0 = (N!)^{-1/2} \sum_{a=1}^{N!} (-1)^a \hat{P}_a \{\chi_1(\vec{s}_1)\chi_2(\vec{s}_2)\ldots\chi_K(\vec{s}_N)\}, \tag{4}$$

where $\hat{P}$ is the permutation operator for N electrons, and the parity of these permutations is attributed to the term $(-1)^a$.

Since we are considering the UHF method, we have taken into account in the calculation the spin of each molecular electron [45]. For an open-shell system, the spin-orbitals are differentiated by the up or down states,

$$\chi(s) = \begin{cases} \psi^\alpha(\vec{r})\ \alpha(\omega) \\ \psi^\beta(\vec{r})\ \beta(\omega) \end{cases}, \tag{5}$$

where $s = \{\vec{r}, \omega\}$ ensembles the spatial $\vec{r}$ and spin ω coordinates. Therefore, the electrons with α and β spins are described by different spatial functions, this spatial freedom being the core idea of an unrestricted formulation. Considering that an unrestricted singlet collapses to a restricted singlet (no unpaired electrons) system, if $\{\psi^\alpha\} \equiv \{\psi^\beta\}$, a method embedded by an unrestricted description of the molecular wave function unveils the possibility of calculating any spin angular momentum state system.

Considering the fundamental concepts presented above, in the next three subsections, the basic mathematical details of the formulation are shown in a summarized way. A complete and detailed exposition of the analytic procedure is addressed in a proper companion paper.

2.1 | Nuclear scattering amplitude

Considering the nuclear component of the scattering amplitude (2) and the description of the system wavefunction (3), it reads:

$$\mathcal{F}_{nuc} = -q\frac{1}{2\pi} \sum_{A=1}^{M} \mathcal{Z}_A \int d^3\vec{x} \frac{e^{i(\vec{k}_i-\vec{k}_f)\cdot\vec{x}}}{|\vec{x} - \vec{R}_A|} \tag{6}$$

where we are considering the normalization of the plane wave as $\langle\vec{x}|\vec{k}\rangle = (2\pi)^{-3/2}e^{i\vec{k}\cdot\vec{x}}$. In order to evaluate this amplitude, the denominator part of the potential can be rewritten taking into account the expression

$$\frac{1}{|\vec{x} - \vec{r}|} = \frac{1}{2\pi^2} \int \frac{d^3\vec{p}}{p^2}\ e^{i\vec{p}\cdot\vec{x}}\ e^{-i\vec{p}\cdot\vec{r}}. \tag{7}$$

Rewriting, then, the nuclear amplitude (6) with Eq. (7), one can readily identify the Fourier transform of the plane wave. After some manipulation and considering the sifting property of the Dirac delta function, the nuclear amplitude results in

$$\mathcal{F}_{nuc} = -2q \sum_{A=1}^{M} \mathcal{Z}_A \frac{e^{-i(\vec{k}_f-\vec{k}_i)\cdot\vec{R}_A}}{(\vec{k}_f - \vec{k}_i)^2}. \tag{8}$$

When the molecule's center of mass is at the origin of the Cartesian coordinate system (both laboratory and
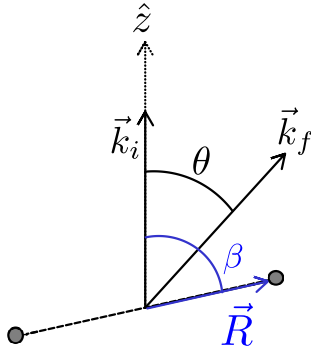
FIGURE 1 Pictorial description of the wavevectors and the molecular system. Initial and final wavevectors are represented, respectively, by $\vec{k}_i$ and $\vec{k}_f$. Since the molecular charge distribution is invariant regarding the azimuth Euler angle α, the scattering azimuth angle ϕ has the same value, i.e., $\phi = \alpha$, and are omitted in the figure.

molecular frames), without loss of generality, the incident particle (or incident beam) can be considered to be in the $\hat{z}$ axis, thus $\vec{k}_i = k\hat{z}$. In such system, the direction of the wave vector of the scattered particle ($\vec{k}_f$) is identified by two angles (θ, ϕ), which readily characterize the scattering angle distribution. Since we are dealing with homonuclear diatomic molecules, the molecular orientation can be defined by a vector that locates one of the atomic centers $\vec{R}$, see Fig. 1. As commented before, for such class of molecules two Euler angles are needed (β, α), related to the polar and azimuth descriptions respectively. That being said, the nuclear amplitude for homonuclear diatomic molecules is given by

$$\mathcal{F}_{nuc}(\theta; \beta) = \frac{-q\mathcal{Z}}{k^2 \sin^2 \frac{\theta}{2}} \cos\left[kR\left(-2\sin^2\frac{\theta}{2}\cos\beta + \sin\theta\sin\beta\right)\right] . \tag{9}$$

It is important to notice that due to symmetry the nuclear amplitude does not depend on the azimuth coordinates ϕ and α since the molecular charge distribution is invariant regarding the azimuth angle α. Therefore, the amplitude that originally would be a function of all the polar and azimuth coordinates $\mathcal{F}_{nuc}(\theta, \phi; \beta, \alpha)$ becomes $\mathcal{F}_{nuc}(\theta; \beta)$.

2.2 | Electronic scattering amplitude

In order to describe the molecular orbitals we have used the linear combination of atomic orbitals (LCAO) method considering the approximation of the Gaussian-type orbitals. This technique has its origin in quantum chemistry [46, 47] and has been widely used in molecular physics. This representation of the electron orbitals in the molecule greatly simplifies the calculation due to the product Gaussian theorem. In addition, we have considered Cartesian Gaussian functions (CGF) with the purpose to obtain analytical expressions to the integrals [48] and to possibly extend these calculations to polyatomic systems.

The electronic scattering amplitude (2) can be calculated considering the homogeneous solution (3) and the Slater determinant description of electronic wave function (4). After the manipulations involving the Slater determinant representation, the electronic amplitude can be written as,

$$\mathcal{F}_{elec} = q\frac{1}{2\pi} \int d^4s \sum_{u=1}^{K} \chi_u^*(s) \left(\int d^3\vec{x} \frac{e^{-i(\vec{k}_f - \vec{k}_i)\cdot\vec{x}}}{|\vec{x} - \vec{r}|} \right) \chi_u(s). \tag{10}$$

As commented before, the element $d^4s = d^3\vec{r}\,d\omega$ includes an integration over spin coordinates, such evaluation regarding the spin ω mathematically distinguishes the up and down components of the electronic amplitude. Therefore, the K orbitals are now separated into up and down [2], i.e. there is a split in the u orbital summation considering $K = K_\alpha + K_\beta$, with their own spatial definition:

$$\mathcal{F}_{elec} = \frac{q}{2\pi}\int d^3\vec{r}\sum_{u=1}^{K_\alpha}\psi_u^{\alpha*}(\vec{r})\left(\int d^3\vec{x}\frac{e^{-i(\vec{k}_f-\vec{k}_i)\cdot\vec{x}}}{|\vec{x}-\vec{r}|}\right)\psi_u^{\alpha}(\vec{r}) + \frac{q}{2\pi}\int d^3\vec{r}\sum_{u=1}^{K_\beta}\psi_u^{\beta*}(\vec{r})\left(\int d^3\vec{x}\frac{e^{-i(\vec{k}_f-\vec{k}_i)\cdot\vec{x}}}{|\vec{x}-\vec{r}|}\right)\psi_u^{\beta}(\vec{r}). \quad (11)$$

The spatial orbitals find their representation in the expansion by a set of Cartesian Gaussian functions ($\mathcal{G}_\mu$). Naming μ as the level of the Cartesian Gaussian function (s, p, d and on) and T the center in which the Gaussian is located, the spatial function of the u-th orbital can be written as

$$\psi_u^{\alpha/\beta}(\vec{r}) = \sum_\mu\sum_T C_{u\,\mu}^{T\,\alpha/\beta}\;\mathcal{G}_\mu(\vec{R}_T;\vec{r})\;, \quad (12)$$

where the $C_{u\,\mu}^{T\,\alpha/\beta}$ is the expansion coefficient. It is worth noting that in the expansion (12), the spin information is encapsulated in the coefficient $C_{u\,\mu}^{T\,\alpha}$. The aforementioned μ label will leads to several terms depending on the order of the CGF. If one chooses to incorporate up to f type functions, this summation will reads $\sum_\mu = \sum_{\mu=1}^{\#S}+\sum_{\mu=1}^{\#P}+\sum_{\mu=1}^{\#D}+\sum_{\mu=1}^{\#F}$, causing the number of terms to be evaluated to increase rapidly. For the sake of simplicity, the compact notation $(\sum_\mu)$ will continue to be used.

In the particular case of homonuclear diatomic molecules, since there are two symmetric centers ($\vec{R}_1 = \vec{R}$ and $\vec{R}_2 = -\vec{R}$), these molecular orbitals with up spin configuration are represented by

$$\psi_u^{\alpha}(\vec{r}) = \sum_\mu C_{u\,\mu}^{1\,\alpha}\;\mathcal{G}_\mu(\vec{R}_1;\vec{r}) + \sum_\mu C_{u\,\mu}^{2\,\alpha}\;\mathcal{G}_\mu(\vec{R}_2;\vec{r})\;. \quad (13)$$

The mathematical expression to the μ−th Cartesian Gaussian function centered in $\vec{R}_T$ has the usual representation [48],

$$\mathcal{G}_\mu(\vec{R}_T;\vec{r}) = N_\mu(\epsilon_\mu,l_\mu,m_\mu,n_\mu)\,(x-X_T)^{l_\mu}\,(y-Y_T)^{m_\mu}\,(z-Z_T)^{n_\mu}\,e^{-\epsilon_\mu|\vec{r}-\vec{R}_T|^2}\;, \quad (14)$$

with normalization generally given as a function of the exponent (ϵ) and the pseudo-quantum numbers (l, m and n),

$$N(\epsilon,l,m,n) = \left[\frac{2^{2(l+m+n)+\frac{3}{2}}\,\epsilon^{l+m+n+\frac{3}{2}}}{(2l-1)!!(2m-1)!!(2n-1)!!\,\pi^{\frac{3}{2}}}\right]^{\frac{1}{2}}. \quad (15)$$

In order to calculate the electronic amplitude (11) we have considered the expression (7), as done before, to rewrite the electrostatic potential. After evaluating both integrations in the incident particle ($d^3\vec{x}$) and the auxiliary vector ($d^3\vec{p}$), one can find the general form to the electronic amplitude for up spin molecular electrons as,

$$\mathcal{F}_{elec}^{\alpha} = \frac{2q}{(\vec{k}_f-\vec{k}_i)^2}\sum_{u=1}^{K_\alpha}\sum_{\mu,\nu}\sum_{T,Q=1}^{2}C_{u\,\mu}^{T\,\alpha}C_{u\,\nu}^{Q\,\alpha}\int d^3\vec{r}\,e^{-i(\vec{k}_f-\vec{k}_i)\cdot\vec{r}}\;\mathcal{G}_\mu(\vec{R}_T;\vec{r})\,\mathcal{G}_\nu(\vec{R}_Q;\vec{r})\;, \quad (16)$$

[2] Alternatively, for simplicity, one can consider the odd and even values of the u-th orbitals as up and down respectively, i.e. $\chi_{odd}(s) = \psi^{\alpha}(\vec{r})\,\alpha(\omega)$ and $\chi_{even}(s) = \psi^{\beta}(\vec{r})\,\beta(\omega)$.

where the v and Q labels are related to the complex conjugate of the spatial orbital (12). The summation in μ and v has been left without upper limits since it depends on the number and type of Gaussian functions used in the calculation, as commented before.

The integration involving the product of Gaussian functions has analytical form [48], in fact, considering the product Gaussian theorem, such integration is basically a Fourier transform of the resulting Gaussian function.

The analogous expression of (16) for molecular electrons with down spin configuration, *i.e.* $\mathcal{F}_{elec}^{\beta}$, can be obtained with a similar procedure as presented here. Therefore, the electronic scattering amplitude is simply the sum of these two terms, thus $\mathcal{F}_{elec} = \mathcal{F}_{elec}^{\alpha} + \mathcal{F}_{elec}^{\beta}$. Finally, the scattering amplitude can be written considering the nuclear and electronic parts as $\mathcal{F} = \mathcal{F}_{nuc} + \mathcal{F}_{elec}^{\alpha} + \mathcal{F}_{elec}^{\beta}$ in its full form .

2.3 | Differential cross sections and computational details

It is important to remember that the scattering amplitude presented above are a function of the scattering angles (θ, ϕ) and the Euler angles (β, α) that describe the orientation of the molecule. As commented before, due to the symmetry of the system, our DCS's are only explicitly dependent on the polar coordinates $(\theta; \beta)$. Mathematically, it means that the DCS of aligned homonuclear diatomic molecules is computed as

$$\frac{d^4\sigma}{d\theta d\phi d\beta d\alpha}(\theta; \beta) = |\mathcal{F}(\theta, \phi; \beta, \alpha)|^2 = |\mathcal{F}_{nuc} + \mathcal{F}_{elec}|^2 \ . \tag{17}$$

The DCS as measured in the experiment, *i.e.*, taking into account an average in the orientation of the molecule, mathematically reads

$$\frac{d^2\sigma}{d\theta d\phi}(\theta) = \frac{1}{4\pi}\int_0^{2\pi} d\alpha \int_0^{\pi} d\beta \ \sin\beta \ |\mathcal{F}(\theta, \phi; \beta, \alpha)|^2 \ . \tag{18}$$

The dimensionless constant q that distinguishes positrons and electrons, present in the interacting potential (1), has no effect is the final DCS expression due to the squared modulus of the scattering amplitude, making these results suitable for both positrons and electrons impact. This situation shall readily change if polarization effects are incorporated in the model.

The expansion coefficients used in the representation of the spacial orbitals, see Eqs.(12) and (13), were calculated through an UHF method. For the $^3\sum_g^-$ ground state wavefunction of molecular oxygen we have applied the Gaussian basis set used in Tenfen *et al.* [49] with uncontracted exponents adding an f-type function (with exponent equal to 0.01).

As shown in Table 1, the basis set employed in the O_2 calculations gives a ground state energy to the triplet state of -149.66 Hartree (E_h) and electric quadrupole moment of $-0.286 \ ea_0^2$, in good agreement with multireference averaged coupled pair functional data [58, 52] and experimental [59, 60] measurements. The static dipole polarizabilities, $\alpha_{\parallel} = 17.85 \ e^2 a_0^2/E_h$ and $\alpha_{\perp} = 5.379 \ e^2 a_0^2/E_h$, are similar to previously reported results [61, 50].

For the N_2 scattering we have applied the same basis set as in a previous calculation [62] for this system performed by our group in rotational excitation calculations, however with uncontracted exponents. The UHF ground state energy value $-108.98 \ E_h$ is close to previous reported data[50, 63], likewise the static dipole polarizabilities $\alpha_{\parallel} = 14.92$ $e^2 a_0^2/E_h$ and $\alpha_{\perp} = 9.503 \ e^2 a_0^2/E_h$ are in accordance with previous *ab initio* calculations[50]. The quadrupole moment of $-0.937 \ ea_0^2$ is also in agreement with previous theoretical [53, 64] and experimental[65] values. In the H_2 case, we have used basis set B from Zanin *et al.* [66] in our UHF calculation. These authors presented a complete analysis regarding molecular property values. Our results are similar to the theoretical [51, 54, 56, 64, 67, 68] and experimental

TABLE 1 Ground state energy (E_0), electric quadrupole moment (Q), longitudinal and transverse static dipole polarizabilities ($\alpha_\parallel$ and $\alpha_\perp$) and equilibrium internuclear distance ($2R$) values obtained in this work compared to other data available in literature. All values are given in atomic units.

Property	O$_2$		N$_2$		H$_2$	
	This work	Ref.	This work	Ref.	This work	Ref.
E_0	-149.66	-149.66 [50]	-108.98	-108.99 [50]	-1.13362	-1.13363 [51]
Q	-0.286	-0.225 [52]	-0.937	-0.940 [53]	0.493	0.487 [54]
$\alpha_\parallel$	17.85	17.88 [50]	14.92	14.72 [55]	6.449	6.380 [56]
$\alpha_\perp$	5.379	7.82 [50]	9.503	10.06 [55]	4.605	4.578 [56]
$2R$	2.28 [57]		2.07 [57]		1.40 [57]	

[69] values for the properties described in Table 1.

In the scattering process of electrons by open-shell systems the coupling of spin must always be addressed. The molecular oxygen has three low-lying states ($^3\Sigma_g^-$, $^1\Delta_g$ and $^1\Sigma_g^+$)[3] due to a π ground state electronic configuration [70, 71]. Since the incident electron is in either up or down states, the coupling of the incident electron and molecular ones yields final total spin configurations of $3/2$ and $1/2$. In that case, the DCS is obtained performing a statistical average in both states [72, 73], *i.e.* a weighted sum of the quartet and doublet spin components.

In the present calculation, the electron-O$_2$ interaction is treated with the molecule in the triplet ground state, since it is the lowest state, energetically, and more abundant and stable by the experimental point of view. The Hamiltonian considered here does not include the exchange interaction or any spin-dependent term [74, 75], hence it is not possible to distinguish the scattering process with final configuration of spin $3/2$ and $1/2$, consequently no average in states is needed in this level of approximation at the present moment.

3 | RESULTS AND DISCUSSION

In the scattering process, when diatomic molecules are considered to be in an aligned orientation ensemble certain Young type interference patterns are present in the DCS [33, 35]. Monitoring the values of the nuclear and electronic amplitudes, it is possible to observe, mathematically, their origins. In Fig. 2, we exhibit the nuclear and electronic amplitudes of H$_2$ by positron impact at 100 eV for perpendicular and parallel orientations. The nuclear part, represented by solid purple line, has its oscillating characteristic due to the trigonometric functions in Eq. (9). Both the nuclear and the electronic amplitude, in purple and solid orange lines, respectively, have similar values in magnitude towards low angles but distinct behavior after 60 degrees.

The DCS of the molecule perpendicularly (left) and parallel (right) aligned to the incident beam is shown in Fig. 2 in dotted line with logarithm scale (label in the right side of figure). The results are obtained as described in Eq. (17). Since the total amplitude is given by the superposition of the nuclear and electronic parts, the minima observed in the cross section are present when both have the same absolute value, *i.e.* $|\mathcal{F}_{nuc}| = |\mathcal{F}_{elec}|$.

As commented in the previous section, due to the distribution of charge density in diatomic molecules the results for the DCSs are independent on the azimuth angles. In fact, since we are considering the incident particle in the $\hat{z}$

---

[3]The two singlet states $^1\Delta_g$ and $^1\Sigma_g^+$ of O$_2$ are also called metastable singlet oxygen due to the small lifetime compared to the triplet one.
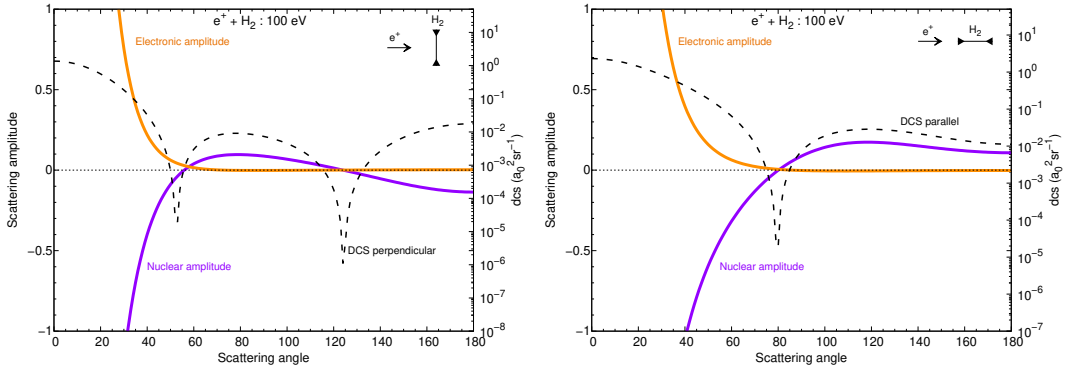
FIGURE 2 Scattering amplitude (left vertical axis) and elastic differential cross section (right vertical axis) of H_2 by lepton impact with incident energy of 100 eV, in this process the molecule is aligned perpendicularly (left) and parallel (right) to the incident particle. Solid lines with labels are the nuclear and electronic amplitudes. The resulting differential cross section is shown in dotted line.
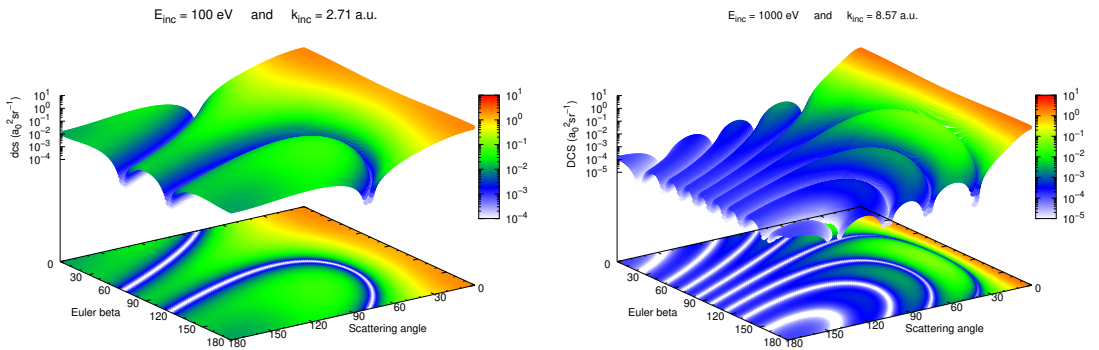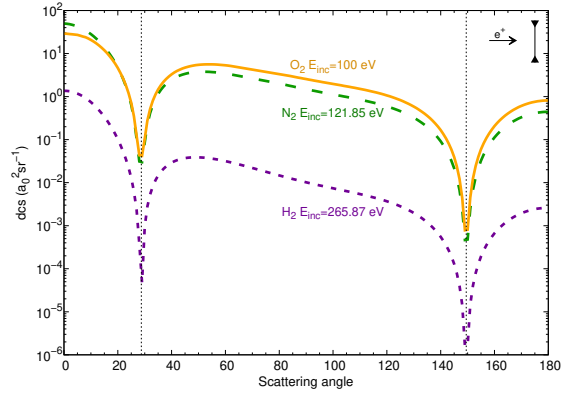

FIGURE 3 Differential cross section of positrons/electrons by H_2 for 100 eV and 1 keV. The 3D plot shows the dependency of the DCS with the scattering angle θ and the Euler angle β. It is possible to see the increase in the minima patterns with the incident energy.

axis, both azimuthal angles have the same values, *i.e.*, the azimuth related to the scattered particle (ϕ) and the Euler angle (α) are equal. In the mathematical development of the expressions, such equality leads to the Pythagorean trigonometric identity[4], taking out the azimuth information of the final expression. If one considers the molecule fixed in the $\hat{z}$ axis ($\vec{R} = R\hat{z}$) instead of the incident particle, the previous comment would be still valid, however the azimuth angles would be the ones related to the incident (ϕ_i) and scattered particle (ϕ_f). In fact, it is advised to perform

---

[4]The Pythagorean identity express the Pythagorean theorem in terms of the trigonometric functions sine and cosine: $\cos^2\theta + \sin^2\theta = 1$.

FIGURE 4 DCS of H_2 (dotted purple), N_2 (dashed green) and O_2 (solid orange) by lepton impact. In this process the molecule is aligned perpendicularly to the incident particle. The same pattern of young-type interference is obtained for the different species when the ratio of the molecular diameter and wavelength of the incident particle are identical.

the calculation in both configurations ($\vec{k}_i$ or $\vec{R}$ fixed in the $\hat{z}$ axis), It will assure that the result and the definition of the angles are correct. We emphasize that the choice is only relevant to simplify a few steps in the calculation and the results in both configurations are the same.

In Fig. 3 the DCS for H_2 is shown as a function of the scattering angle (θ) and the polar Euler angle (β). The fact that the DCS is the same for $\beta = 0°$ and $\beta = 180°$ along with the fact that the geometric description of the scattering process to the molecules with $\beta = 60°$ and $\beta = 120°$ is the same could lead one to believe that the result would be symmetric to $\beta = 90°$. However, as seen for 100 eV and 1 keV the minima patterns are not symmetric regarding the euler angle β. It can be explained observing the argument of the cosine function in Eq. (9), where the term $-2\sin^2 \frac{\theta}{2}$ works as a "weight function" to the distribution of probability in the scattering process, breaking the symmetry in β.

The evolution of the DCS regarding the energy of the incident particle is shown in the supplementary material. It is possible to observe the isotropic nature of the DCS for very low energies. At this energy regime (when $k \to 0$) the scattering process is dominated by the S-wave and it is possible to relate the scattering amplitude directly to the scattering length [76].

Considering a classical wave mechanics view, since the minima in the aligned DCS comes from the interference between the scattered waves from each molecular center, such phenomenon can be explained through a phase shift analysis of independent scattering centers [35]. Noticing the distinction in the path of both waves, the phase difference leads to oscillatory functions similar to the one in the nuclear amplitude (9). Examining the same classical view, the minima patterns in the scattering process of a perpendicular molecule can only be observed when the molecular diameter is compatible with the wavelength of the incident particle.

In figure 4, we present the DCSs of H_2, N_2 and O_2 with the molecules perpendicularly oriented ($\beta = 90°$). The Young-type pattern observed in the scattering is strongly connected to the wavelength of the incident particle and the molecular internuclear distance. In order to see that, we display in this figure three systems in which the ratio of these quantities is the same, *i.e.*,

$$\left(\frac{2R}{\lambda_{inc}}\right)_{H_2} = \left(\frac{2R}{\lambda_{inc}}\right)_{N_2} = \left(\frac{2R}{\lambda_{inc}}\right)_{O_2} . \tag{19}$$

The presence of the same pattern in different systems exemplify the analogy of diatomic homonuclear molecules to the double-slit experiment. It is important to notice that this is only achieved due to the simple approximations applied to this model. The particle wavefunction is taken in the FBA, the scattering potential is the static one and, most importantly, the calculation is done in a fixed nuclei approximation, *i.e.* the vibrational and rotational effects are
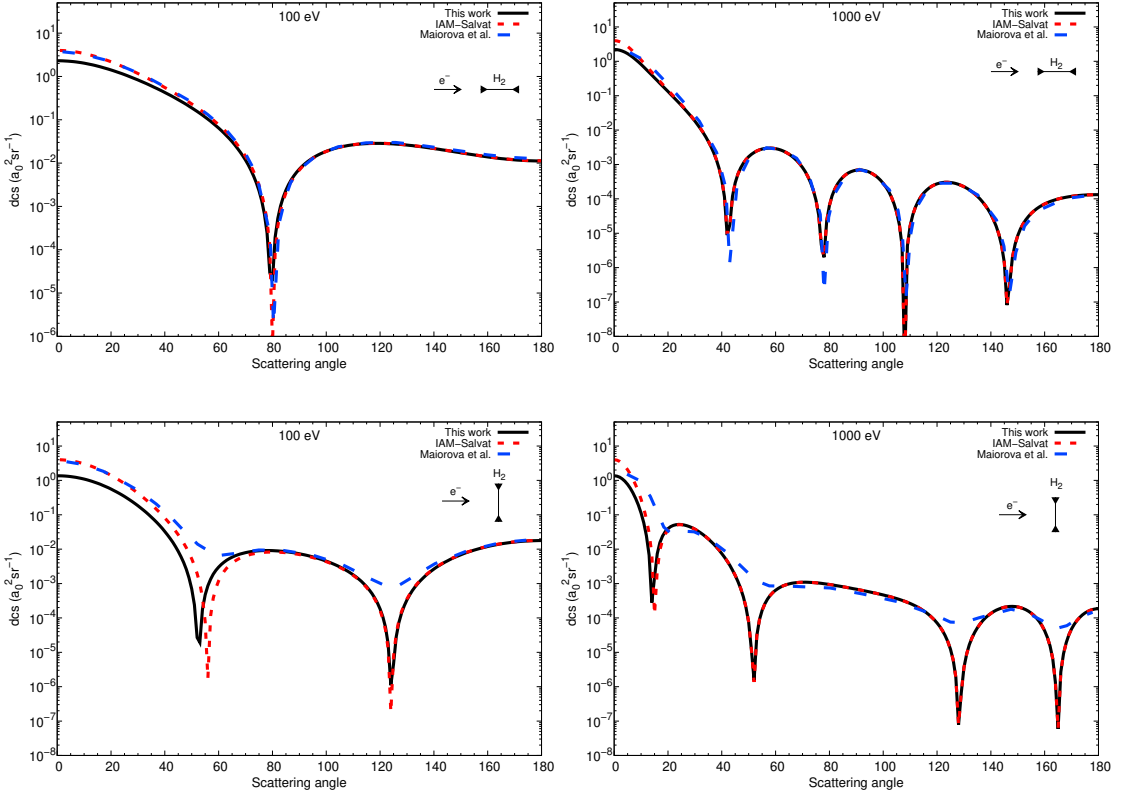
neglected.

FIGURE 5 Differential cross section of H_2 by positrons/electrons. In the top set of DCS's the molecule is parallel oriented to the incident particle, top left with incident energy of 100 eV, top right 1 keV, as indicated in labels. The bottom set shows the scattering for a molecule perpendicularly oriented to the incident particle, energies are the same as the top set. Solid line, our results; dashed blue line, Maiorova *et al.* [35]; dotted red line are results obtained with the IAM-Salvat results [37, 77, 38].

In addition to our *ab initio* results, we have performed a calculation considering the scattering amplitude given by the form factors of Salvat *et al.* [77, 78] combined with the independent atom model [37, 38] taking the incident particle as a regular plane wave. In the electronic scattering amplitude the charge density comes from a screening function with parameters determined *via* an analytical fitting procedure to Dirac-Hartree-Fock-Slater self-consistent data, such values are available in table 1 of reference [77]. After that, the DCS for aligned molecules is computed through the independent atom model, referred in this manuscript as IAM-Salvat.

In Fig. 5, we compare our *ab initio* results (solid line) with the calculation of Maiorova *et al.* (dashed blue line) [35] (with twisted electrons) and the IAM-Salvat model (dotted red line). The magnitude difference for low angles is due to the different level of description of the electronic density charge within the models. As stated before, the electronic amplitude plays a major role in the low angle region. Since we have used an *ab initio* representation and both Maiorova

and IAM-Salvat results are performed with form factors the small magnitude difference was expected.

In the perpendicular scenario, bottom row of Fig. 5, the aforementioned descriptions of the electronic charge densities are responsible for the shift in the minima towards low angles. As the electronic amplitude changes for each model, the angular values when $|\mathcal{F}_{nuc}| = |\mathcal{F}_{elec}|$ alter likewise. Further, the twisted electrons formulation seems to modify the interference pattern experienced by the regular plane wave description, specially the magnitude of the minima. It is plausible, once the incident wavefunction is not the same the interference should result in a different behavior to the DCS.

For high energy scattering (1 keV), despite the difference in magnitude in the low angle region, the IAM-Salvat and the *ab initio* models exhibit basically the same angular values to the minima. In fact, for such energy the wavelength of the incident particle is so small when compared to the internuclear distance ($2R$), that the IAM becomes a very good approximation.

The scattering process when the molecule is parallel aligned to the incident beam is shown in top row of Fig. 5. Results show that the DCS's obtained through *ab initio*, IAM-Salvat and twisted electron models are practically the same. It makes sense when we realize that in this configuration, the charge density along the molecular axis do not have any significant contribution to the scattering process and so the incident electron, being twisted or not, will scatter in the same way. In this configuration, classically thinking, the particle experience consecutive scattering processes,while, on the other hand, when the molecule is aligned perpendicularly to the incident particle the scattering in the two centers can be considered simultaneous. This could explain the similarity in the results to the parallel configuration within the models.

4 | CONCLUSIONS

In this work we have reported elastic differential cross section of aligned diatomic homonuclear molecules by positrons and electrons within an *ab initio* formulation. The first Born approximation combined with the static potential interaction, derived from an Unrestricted Hartree-Fock molecular wavefunction, were employed in order to describe the scattering process.

The comparison of our *ab initio* calculation with the recent reported results of Maiorova *et al.* [35] exhibits a slight difference in magnitude in the very low angle regime due to the adopted description of the molecular target. As expected, the Young-type interference patterns (minima) occur in the same angular values, however with different magnitude for perpendicular scattering. Furthermore, the lower angles minima are somewhat dislocated due to the aforementioned description of the molecular target specially for the perpendicular scattering with the particle at 100 eV incident energy.

Regarding the origin of such interference patterns, the minima present in the differential cross sections are strongly connected to the angular values in which the summation of the nuclear and electronic scattering amplitudes cancel each other. This analysis also shows that different levels of representation of the molecular target, *i.e.* distinct molecular electronic descriptions, lead to particular values to the minima for low angles, where the electronic amplitude contributes the most.

As stated before, all these calculations consider only the static potential and are carried out in the fixed nuclei approximation. Since the Young-type patterns come from the interference between the scattered particles of the two molecular centers, a change in the description of the interacting potential, *i.e.* inclusion of other effects like correlation-polarization and exchange, and the consideration of vibrational states of the molecule must alter significantly the observed interference.

Future endeavors include a more complete description of the interaction and an accurate scattered wavefunction. Once these forthcoming objectives are addressed, we will be able to explore in a precise manner a broad range of systems with an *ab initio* formulation, investigating other scattering channels in different energy ranges. The FBA calculation has a crucial importance in the verification, validation and debugging of more complex formulations, since at certain conditions, no matter the complexity of a method, it must give the same outcome as the FBA results.

Acknowledgements

Conflict of interest

The authors declare no conflict of interest.

references

[1] Louis De Broglie. Waves and quanta. *Nature*, 112(2815):540–540, 1923. doi: 10.1038/112540a0.

[2] Thomas Young. I. the bakerian lecture. experiments and calculations relative to physical optics. *Philosophical Transactions of the Royal Society of London*, 94:1–16, 1804. doi: 10.1098/rstl.1804.0001. URL https://royalsocietypublishing.org/doi/abs/10.1098/rstl.1804.0001.

[3] Clinton Joseph Davisson and Lester Halbert Germer. Reflection of electrons by a crystal of nickel. *Proceedings of the National Academy of Sciences of the United States of America*, 14(4):317, 1928. doi: 10.1073/pnas.14.4.317.

[4] H. F. Schouten, N. Kuzmin, G. Dubois, T. D. Visser, G. Gbur, P. F. A. Alkemade, H. Blok, G. W. 't Hooft, D. Lenstra, and E. R. Eliel. Plasmon-assisted two-slit transmission: Young's experiment revisited. *Phys. Rev. Lett.*, 94:053901, Feb 2005. doi: 10.1103/PhysRevLett.94.053901. URL https://link.aps.org/doi/10.1103/PhysRevLett.94.053901.

[5] Razvigor Ossikovski, Oriol Arteaga, Jérémy Vizet, and Enric Garcia-Caurel. On the equivalence between young’s double-slit and crystal double-refraction interference experiments. *J. Opt. Soc. Am. A*, 34(8):1309–1314, Aug 2017. doi: 10.1364/JOSAA.34.001309. URL http://josaa.osa.org/abstract.cfm?URI=josaa-34-8-1309.

[6] Maksim Kunitski, Nicolas Eicke, Pia Huber, Jonas Köhler, Stefan Zeller, Jörg Voigtsberger, Nikolai Schlott, Kevin Henrichs, Hendrik Sann, Florian Trinter, et al. Double-slit photoelectron interference in strong-field ionization of the neon dimer. *Nature communications*, 10(1):1–7, 2019. doi: 10.1038/s41467-018-07882-8.

[7] J. S. Bell. De broglie-bohm, delayed-choice, double-slit experiment, and density matrix. *International Journal of Quantum Chemistry*, 18(S14):155–159, 1980. doi: https://doi.org/10.1002/qua.560180819. URL https://onlinelibrary.wiley.com/doi/abs/10.1002/qua.560180819.

[8] Ciann-Dong Yang and Kuan-Chang Su. Reconstructing interference fringes in slit experiments by complex quantum trajectories. *International Journal of Quantum Chemistry*, 113(9):1253–1263, 2013. doi: https://doi.org/10.1002/qua.24269. URL https://onlinelibrary.wiley.com/doi/abs/10.1002/qua.24269.

[9] Anton Zeilinger, Roland Gähler, C. G. Shull, Wolfgang Treimer, and Walter Mampe. Single- and double-slit diffraction of neutrons. *Rev. Mod. Phys.*, 60:1067–1073, Oct 1988. doi: 10.1103/RevModPhys.60.1067. URL https://link.aps.org/doi/10.1103/RevModPhys.60.1067.

[10] Mario Barbatti, Alexandre B. Rocha, and Carlos E. Bielschowsky. Young-type interference pattern in molecular inner-shell excitations by electron impact. *Phys. Rev. A*, 72:032711, Sep 2005. doi: $10.1103/\mathrm{PhysRevA}.72.032711$. URL `https://link.aps.org/doi/10.1103/PhysRevA.72.032711`.

[11] A S Baltenkov, U Becker, S T Manson, and A Z Msezane. Interference in the molecular photoionization and young's double-slit experiment. *Journal of Physics B: Atomic, Molecular and Optical Physics*, 45(3):035202, jan 2012. doi: $10.1088/0953-4075/45/3/035202$. URL `https://doi.org/10.1088/0953-4075/45/3/035202`.

[12] Yuya Hasegawa, Koh Saitoh, Nobuo Tanaka, Shogo Tanimura, and Masaya Uchida. Young's interference experiment with electron beams carrying orbital angular momentum. *Journal of the Physical Society of Japan*, 82(3):033002, 2013. doi: $10.7566/\mathrm{JPSJ}.82.033002$. URL `https://doi.org/10.7566/JPSJ.82.033002`.

[13] Zehra Nur Ozer, Hari Chaluvadi, Melike Ulu, Mevlut Dogan, Bekir Aktas, and Don Madison. Young's double-slit interference for quantum particles. *Phys. Rev. A*, 87:042704, Apr 2013. doi: $10.1103/\mathrm{PhysRevA}.87.042704$. URL `https://link.aps.org/doi/10.1103/PhysRevA.87.042704`.

[14] O. Carnal and J. Mlynek. Young's double-slit experiment with atoms: A simple atom interferometer. *Phys. Rev. Lett.*, 66:2689–2692, May 1991. doi: $10.1103/\mathrm{PhysRevLett}.66.2689$. URL `https://link.aps.org/doi/10.1103/PhysRevLett.66.2689`.

[15] J. Seifert and H. Winter. Young-type interference for scattering of fast helium atoms from an oxygen covered mo(112) surface. *Phys. Rev. Lett.*, 108:065503, Feb 2012. doi: $10.1103/\mathrm{PhysRevLett}.108.065503$. URL `https://link.aps.org/doi/10.1103/PhysRevLett.108.065503`.

[16] L. Ph. H. Schmidt, S. Schössler, F. Afaneh, M. Schöffler, K. E. Stiebing, H. Schmidt-Böcking, and R. Dörner. Young-type interference in collisions between hydrogen molecular ions and helium. *Phys. Rev. Lett.*, 101:173202, Oct 2008. doi: $10.1103/\mathrm{PhysRevLett}.101.173202$. URL `https://link.aps.org/doi/10.1103/PhysRevLett.101.173202`.

[17] H. Agueny, A. Makhoute, A. Dubois, and J. P. Hansen. Coherent electron emission beyond young-type interference from diatomic molecules. *Phys. Rev. A*, 93:012713, Jan 2016. doi: $10.1103/\mathrm{PhysRevA}.93.012713$. URL `https://link.aps.org/doi/10.1103/PhysRevA.93.012713`.

[18] Saba N. Khan, Stuti Joshi, and P. Senthilkumaran. Young's double-slit experiment with vector vortex beams. *Opt. Lett.*, 46(17):4136–4139, Sep 2021. doi: $10.1364/\mathrm{OL}.434177$. URL `http://ol.osa.org/abstract.cfm?URI=ol-46-17-4136`.

[19] N. Stolterfoht, B. Sulik, V. Hoffmann, B. Skogvall, J. Y. Chesnel, J. Rangama, F. Frémont, D. Hennecart, A. Cassimi, X. Husson, A. L. Landers, J. A. Tanis, M. E. Galassi, and R. D. Rivarola. Evidence for interference effects in electron emission from H_2 colliding with 60MeV/u kr^{34+} ions. *Phys. Rev. Lett.*, 87:023201, Jun 2001. doi: $10.1103/\mathrm{PhysRevLett}.87.023201$. URL `https://link.aps.org/doi/10.1103/PhysRevLett.87.023201`.

[20] M. E. Galassi, R. D. Rivarola, P. D. Fainstein, and N. Stolterfoht. Young-type interference patterns in electron emission spectra produced by impact of swift ions on h$_2$ molecules. *Phys. Rev. A*, 66:052705, Nov 2002. doi: $10.1103/\mathrm{PhysRevA}.66.052705$. URL `https://link.aps.org/doi/10.1103/PhysRevA.66.052705`.

[21] Deepankar Misra, A. Kelkar, U. Kadhane, Ajay Kumar, Lokesh C. Tribedi, and P. D. Fainstein. Influence of young-type interference on the forward-backward asymmetry in electron emission from h$_2$ in collisions with 80–MeV bare c ions. *Phys. Rev. A*, 74:060701, Dec 2006. doi: $10.1103/\mathrm{PhysRevA}.74.060701$. URL `https://link.aps.org/doi/10.1103/PhysRevA.74.060701`.

[22] N. Stolterfoht, B. Sulik, L. Gulyás, B. Skogvall, J. Y. Chesnel, F. Frémont, D. Hennecart, A. Cassimi, L. Adoui, S. Hossain, and J. A. Tanis. Interference effects in electron emission from h$_2$ by 68-mev/u kr^{33+} impact: Dependence on the emission angle. *Phys. Rev. A*, 67:030702, Mar 2003. doi: $10.1103/\mathrm{PhysRevA}.67.030702$. URL `https://link.aps.org/doi/10.1103/PhysRevA.67.030702`.

[23] A. B. Voitkiv, B. Najjari, D. Fischer, A. N. Artemyev, and A. Surzhykov. Young-type interference in projectile-electron loss in energetic ion-molecule collisions. *Phys. Rev. Lett.*, 106:233202, Jun 2011. doi: $10.1103/\mathrm{PhysRevLett}.106.233202$. URL `https://link.aps.org/doi/10.1103/PhysRevLett.106.233202`.

[24] J. S. Alexander, A. C. Laforge, A. Hasan, Z. S. Machavariani, M. F. Ciappina, R. D. Rivarola, D. H. Madison, and M. Schulz. Interference effects due to projectile target nucleus scattering in single ionization of h_2 by 75−keV proton impact. *Phys. Rev. A*, 78:060701, Dec 2008. doi: 10.1103/PhysRevA.78.060701. URL https://link.aps.org/doi/10.1103/PhysRevA.78.060701.

[25] J. L. Baran, S. Das, F. Járai-Szabó, K. Póra, L. Nagy, and J. A. Tanis. Suppression of primary electron interferences in the ionization of n_2 by $1 − 5 MeV$ u protons. *Phys. Rev. A*, 78:012710, Jul 2008. doi: 10.1103/PhysRevA.78.012710. URL https://link.aps.org/doi/10.1103/PhysRevA.78.012710.

[26] Sophie E. Canton, Etienne Plésiat, John D. Bozek, Bruce S. Rude, Piero Decleva, and Fernando Martín. Direct observation of young's double-slit interferences in vibrationally resolved photoionization of diatomic molecules. *Proceedings of the National Academy of Sciences*, 108(18):7302–7306, 2011. ISSN 0027-8424. doi: 10.1073/pnas.1018534108.

[27] N. A. Cherepkov, S. K. Semenov, M. S. Schöffler, J. Titze, N. Petridis, T. Jahnke, K. Cole, L. Ph. H. Schmidt, A. Czasch, D. Akoury, O. Jagutzki, J. B. Williams, T. Osipov, S. Lee, M. H. Prior, A. Belkacem, A. L. Landers, H. Schmidt-Böcking, R. Dörner, and Th. Weber. Auger decay of $1\sigma_g$ and $1\sigma_u$ hole states of the n_2 molecule. ii. young-type interference of auger electrons and its dependence on internuclear distance. *Phys. Rev. A*, 82:023420, Aug 2010. doi: 10.1103/PhysRevA.82.023420. URL https://link.aps.org/doi/10.1103/PhysRevA.82.023420.

[28] K. Kreidi, D. Akoury, T. Jahnke, Th. Weber, A. Staudte, M. Schöffler, N. Neumann, J. Titze, L. Ph. H. Schmidt, A. Czasch, O. Jagutzki, R. A. Costa Fraga, R. E. Grisenti, M. Smolarski, P. Ranitovic, C. L. Cocke, T. Osipov, H. Adaniya, J. C. Thompson, M. H. Prior, A. Belkacem, A. L. Landers, H. Schmidt-Böcking, and R. Dörner. Interference in the collective electron momentum in double photoionization of h_2. *Phys. Rev. Lett.*, 100:133005, Apr 2008. doi: 10.1103/PhysRevLett.100.133005. URL https://link.aps.org/doi/10.1103/PhysRevLett.100.133005.

[29] R. Della Picca, P. D. Fainstein, and A. Dubois. Cooper minima and young-type interferences in the photoionization of H_2^+. *Phys. Rev. A*, 84:033405, Sep 2011. doi: 10.1103/PhysRevA.84.033405. URL https://link.aps.org/doi/10.1103/PhysRevA.84.033405.

[30] T. F. Tuan and E. Gerjuoy. Charge transfer in molecular hydrogen. *Phys. Rev.*, 117:756–763, Feb 1960. doi: 10.1103/PhysRev.117.756. URL https://link.aps.org/doi/10.1103/PhysRev.117.756.

[31] S. A. Alexander, R. L. Coldwell, Ruth E. Hoffmeyer, and Ajit J. Thakkar. High-energy electron and x-ray scattering from h2 using monte carlo techniques. *International Journal of Quantum Chemistry*, 56(S29):627–630, 1995. doi: https://doi.org/10.1002/qua.560560868. URL https://onlinelibrary.wiley.com/doi/abs/10.1002/qua.560560868.

[32] S Chatterjee, S Kasthurirangan, A H Kelkar, C R Stia, O A Fojón, R D Rivarola, and L C Tribedi. Fast-electron impact ionization of molecular hydrogen: energy and angular distribution of double and single differential cross sections and young-type interference. *Journal of Physics B: Atomic, Molecular and Optical Physics*, 42(6):065201, mar 2009. doi: 10.1088/0953-4075/42/6/065201. URL https://doi.org/10.1088/0953-4075/42/6/065201.

[33] Ajit J. Thakkar, A. N. Tripathi, and Vedene H. Smith. Molecular x-ray- and electron-scattering intensities. *Phys. Rev. A*, 29:1108–1113, Mar 1984. doi: 10.1103/PhysRevA.29.1108. URL https://link.aps.org/doi/10.1103/PhysRevA.29.1108.

[34] Junfang Gao, D. H. Madison, and J. L. Peacher. Interference effects for low-energy electron-impact ionization of nitrogen molecules. *Phys. Rev. A*, 72:032721, Sep 2005. doi: 10.1103/PhysRevA.72.032721. URL https://link.aps.org/doi/10.1103/PhysRevA.72.032721.

[35] A. V. Maiorova, S. Fritzsche, R. A. Müller, and A. Surzhykov. Elastic scattering of twisted electrons by diatomic molecules. *Phys. Rev. A*, 98:042701, Oct 2018. doi: 10.1103/PhysRevA.98.042701. URL https://link.aps.org/doi/10.1103/PhysRevA.98.042701.

[36] D. V. Karlovets, G. L. Kotkin, V. G. Serbo, and A. Surzhykov. Scattering of twisted electron wave packets by atoms in the born approximation. *Phys. Rev. A*, 95:032703, Mar 2017. doi: 10.1103/PhysRevA.95.032703. URL https://link.aps.org/doi/10.1103/PhysRevA.95.032703.

[37] M. K. Srivastava, A. N. Tripathi, and Mohan Lal. Exchange effects in the independent-atom model of electron-molecule scattering. *Phys. Rev. A*, 18:2377–2378, Nov 1978. doi: 10.1103/PhysRevA.18.2377. URL https://link.aps.org/doi/10.1103/PhysRevA.18.2377.

[38] Haruhide Miyagi, Toru Morishita, and Shinichi Watanabe. Electron scattering and photoionization of one-electron diatomic molecules. *Phys. Rev. A*, 85:022708, Feb 2012. doi: 10.1103/PhysRevA.85.022708. URL https://link.aps.org/doi/10.1103/PhysRevA.85.022708.

[39] A.Lewis Ford and J.C. Browne. Elastic scattering of electrons by h2 in the born approximation. *Chemical Physics Letters*, 20(3):284–290, 1973. ISSN 0009-2614. doi: https://doi.org/10.1016/0009-2614(73)85178-4. URL https://www.sciencedirect.com/science/article/pii/0009261473851784.

[40] M Inokuti and M R C McDowell. Elastic scattering of fast electrons by atoms. i. helium to neon. *Journal of Physics B: Atomic and Molecular Physics*, 7(17):2382–2395, dec 1974. doi: 10.1088/0022-3700/7/17/024. URL https://doi.org/10.1088/0022-3700/7/17/024.

[41] J. W. Liu. Elastic scattering of fast electrons by $h_2(^1\Sigma_g^+)$ and $n_2(x^1\Sigma_g^+)$. *Phys. Rev. A*, 32:1384–1394, Sep 1985. doi: 10.1103/PhysRevA.32.1384. URL https://link.aps.org/doi/10.1103/PhysRevA.32.1384.

[42] B van Wingerden, F J de Heer, E Weigold, and K J Nygaard. Elastic scattering of electrons by molecular and atomic hydrogen. *Journal of Physics B: Atomic and Molecular Physics*, 10(7):1345–1362, may 1977. doi: 10.1088/0022-3700/10/7/023. URL https://doi.org/10.1088/0022-3700/10/7/023.

[43] Grigoriĭ Drukarev. *Collisions of electrons with atoms and molecules*.

[44] D A Varshalovich, A N Moskalev, and V K Khersonskii. *Quantum Theory of Angular Momentum*. WORLD SCIENTIFIC, 1988. doi: 10.1142/0270. URL https://www.worldscientific.com/doi/abs/10.1142/0270.

[45] Attila Szabo and Neil S Ostlund. *Modern quantum chemistry: introduction to advanced electronic structure theory*. McGraw-Hill Publishing Company, New York, 1989.

[46] S. F. Boys and Alfred Charles Egerton. Electronic wave functions - i. a general method of calculation for the stationary states of any molecular system. *Proceedings of the Royal Society of London. Series A. Mathematical and Physical Sciences*, 200(1063):542–554, 1950. doi: 10.1098/rspa.1950.0036. URL https://royalsocietypublishing.org/doi/abs/10.1098/rspa.1950.0036.

[47] J. E. Lennard-Jones. The electronic structure of some diatomic molecules. *Trans. Faraday Soc.*, 25:668–686, 1929. doi: 10.1039/TF9292500668. URL http://dx.doi.org/10.1039/TF9292500668.

[48] Hiroshi Taketa, Sigeru Huzinaga, and Kiyosi O-ohata. Gaussian-expansion methods for molecular integrals. *Journal of the Physical Society of Japan*, 21(11):2313–2324, 1966. doi: 10.1143/JPSJ.21.2313. URL https://doi.org/10.1143/JPSJ.21.2313.

[49] Wagner Tenfen, Marcos V. Barp, and Felipe Arretche. Low-energy elastic scattering of positrons by o2. *Phys. Rev. A*, 99:022703, Feb 2019. doi: 10.1103/PhysRevA.99.022703. URL https://link.aps.org/doi/10.1103/PhysRevA.99.022703.

[50] Dirk Spelsberg and Wilfried Meyer. Static dipole polarizabilities of n2, o2, f2, and h2o. *The Journal of Chemical Physics*, 101(2):1282–1288, 1994. doi: 10.1063/1.467820. URL https://doi.org/10.1063/1.467820.

[51] W. Kolos and C. C. J. Roothaan. Accurate electronic wave functions for the h2 molecule. *Rev. Mod. Phys.*, 32:219–232, Apr 1960. doi: 10.1103/RevModPhys.32.219. URL https://link.aps.org/doi/10.1103/RevModPhys.32.219.

[52] Massimiliano Bartolomei, Estela Carmona-Novillo, Marta I. Hernández, José Campos-Martínez, and Ramón Hernández-Lamoneda. Long-range interaction for dimers of atmospheric interest: dispersion, induction and electrostatic contributions for o2-o2, n2-n2 and o2-n2. *Journal of Computational Chemistry*, 32(2):279–290, 2011. doi: https://doi.org/10.1002/jcc.21619. URL https://onlinelibrary.wiley.com/doi/abs/10.1002/jcc.21619.

[53] Dage Sundholm, Pekka Pyykkö, and Leif Laaksonen. Two-dimensional, fully numerical molecular calculations. *Molecular Physics*, 56(6):1411–1418, 1985. doi: 10.1080/00268978500103131. URL https://doi.org/10.1080/00268978500103131.

[54] Geerd HF Diercksen and Andrzej J Sadlej. Finite-field many-body perturbation theory iv. basis set optimization in mbpt calculations of molecular properties. molecular quadrupole moments. *Theoretica chimica acta*, 63(1):69–82, 1983. doi: 10.1007/BF00549156.

[55] Stephen R. Langhoff, Charles W. Bauschlicher, and Delano P. Chong. Theoretical study of the effects of vibrational-rotational interactions on the raman spectrum of n2. *The Journal of Chemical Physics*, 78(9):5287–5292, 1983. doi: 10.1063/1.445482. URL https://doi.org/10.1063/1.445482.

[56] W. Kolos and L. Wolniewicz. Polarizability of the hydrogen molecule. *The Journal of Chemical Physics*, 46(4):1426–1432, 1967. doi: 10.1063/1.1840870. URL https://doi.org/10.1063/1.1840870.

[57] William M Haynes. *CRC handbook of chemistry and physics*. CRC press, 2014.

[58] Miroslav Medved, Miroslav Urban, Vladimir Kello, and Geerd H.F. Diercksen. Accuracy assessment of the rohf — ccsd(t) calculations of static dipole polarizabilities of diatomic radicals: O2, cn, and no. *Journal of Molecular Structure: THEOCHEM*, 547(1):219–232, 2001. ISSN 0166-1280. doi: https://doi.org/10.1016/S0166-1280(01)00472-9. URL https://www.sciencedirect.com/science/article/pii/S0166128001004729.

[59] E. Richard Cohen and George Birnbaum. Influence of the potential function on the determination of multipole moments from pressure-induced far-infrared spectra. *The Journal of Chemical Physics*, 66(6):2443–2447, 1977. doi: 10.1063/1.434283. URL https://doi.org/10.1063/1.434283.

[60] A. D. Buckingham, R. L. Disch, and D. A. Dunmur. Quadrupole moments of some simple molecules. *Journal of the American Chemical Society*, 90(12):3104–3107, 1968. doi: 10.1021/ja01014a023. URL https://doi.org/10.1021/ja01014a023.

[61] G.D. Zeiss and William J. Meath. Dispersion energy constants c 6(a, b), dipole oscillator strength sums and refractivities for li, n, o, h2, n2, o2, nh3, h2o, no and n2o. *Molecular Physics*, 33(4):1155–1176, 1977. doi: 10.1080/00268977700100991. URL https://doi.org/10.1080/00268977700100991.

[62] Marcos V Barp, Eliton Popovicz Seidel, Felipe Arretche, and Wagner Tenfen. Rotational excitation of n2 by positron impact in the adiabatic rotational approximation. *Journal of Physics B: Atomic, Molecular and Optical Physics*, 51(20):205201, sep 2018. doi: 10.1088/1361-6455/aade81. URL https://doi.org/10.1088/1361-6455/aade81.

[63] Peter Weinberger and Daniel D. Konowalow. A study of the ground states of n2, o2, and f2 and their esca spectra by the multiple scattering $x\alpha$ method. *International Journal of Quantum Chemistry*, 7(S7):353–367, 1973. doi: https://doi.org/10.1002/qua.560070743. URL https://onlinelibrary.wiley.com/doi/abs/10.1002/qua.560070743.

[64] Donald G. Truhlar. Vibrational matrix elements of the quadrupole moment functions of h2, n2 and co. *International Journal of Quantum Chemistry*, 6(5):975–988, 1972. doi: https://doi.org/10.1002/qua.560060515. URL https://onlinelibrary.wiley.com/doi/abs/10.1002/qua.560060515.

[65] C. GRAHAM D. A. IMRIE R. E. RAAB. Measurement of the electric quadrupole moments of co2, co, n2, cl2 and bf3. *Molecular Physics*, 93(1):49–56, 1998. doi: 10.1080/002689798169429. URL https://doi.org/10.1080/002689798169429.

[66] Guilherme Luiz Zanin, Wagner Tenfen, and Felipe Arretche. Rotational excitation of h 2 by positron impact in adiabatic rotational approximation. *The European Physical Journal D*, 70(9):1–10, 2016. doi: 10.1140/epjd/e2016-70103-0.

[67] Daniel Zeroka. Variation of the polarizability of the hydrogen molecule ion and the hydrogen molecule with internuclear separation. *International Journal of Quantum Chemistry*, 8(1):91–95, 1974. doi: https://doi.org/10.1002/qua.560080110. URL https://onlinelibrary.wiley.com/doi/abs/10.1002/qua.560080110.

[68] David M. Bishop and Janusz Pipin. Dipole, quadrupole, octupole, and dipole–octupole polarizabilities at real and imaginary frequencies for h, he, and h2 and the dispersion-energy coefficients for interactions between them. *International Journal of Quantum Chemistry*, 45(4):349–361, 1993. doi: https://doi.org/10.1002/qua.560450403. URL https://onlinelibrary.wiley.com/doi/abs/10.1002/qua.560450403.

[69] A. D. McLean and M. Yoshimine. Molecular properties which depend on the square of the electronic coordinates; h2 and nno. *The Journal of Chemical Physics*, 45(10):3676–3681, 1966. doi: 10.1063/1.1727387. URL https://doi.org/10.1063/1.1727387.

[70] B. F. Minaev. Intensities of spin-forbidden transitions in molecular oxygen and selective heavy-atom effects. *International Journal of Quantum Chemistry*, 17(2):367–374, 1980. doi: https://doi.org/10.1002/qua.560170219. URL https://onlinelibrary.wiley.com/doi/abs/10.1002/qua.560170219.

[71] Carsten P. Byrman and Joop H. van Lenthe. A valence bond study of the oxygen molecule. *International Journal of Quantum Chemistry*, 58(4):351–360, 1996. doi: https://doi.org/10.1002/(SICI)1097-461X(1996)58:4<351::AID-QUA4>3.0.CO;2-X. URL https://onlinelibrary.wiley.com/doi/abs/10.1002/%28SICI%291097-461X%281996%2958%3A4%3C351%3A%3AAID-QUA4%3E3.0.CO%3B2-X.

[72] L. M. Brescansin, M.-T. Lee, and L. E. Machado. A comparative study on low-energy elastic electron-nhx (x = 1,2,3) collisions. *International Journal of Quantum Chemistry*, 108(13):2312–2317, 2008. doi: https://doi.org/10.1002/qua.21607. URL https://onlinelibrary.wiley.com/doi/abs/10.1002/qua.21607.

[73] KL Baluja and J Singh. Electron scattering with open-shell molecules: R-matrix method. *Indian Journal of Physics*, 85(12):1695–1704, 2011. doi: https://doi.org/10.1007/s12648-011-0182-8.

[74] Jacek Karwowski, Dorota Bielínska-Waż, and Jacek Jurkowski. Eigenvalues of model hamiltonian matrices from spectral density distribution moments: The heisenberg spin hamiltonian. *International Journal of Quantum Chemistry*, 60(1):185–193, 1996. doi: https://doi.org/10.1002/(SICI)1097-461X(1996)60:1<185::AID-QUA20>3.0.CO;2-D. URL https://onlinelibrary.wiley.com/doi/abs/10.1002/%28SICI%291097-461X%281996%2960%3A1%3C185%3A%3AAID-QUA20%3E3.0.CO%3B2-D.

[75] Mohammad Mostafanejad. Basics of the spin hamiltonian formalism. *International Journal of Quantum Chemistry*, 114(22):1495–1512, 2014. doi: https://doi.org/10.1002/qua.24721. URL https://onlinelibrary.wiley.com/doi/abs/10.1002/qua.24721.

[76] Charles Jean Joachain. *Quantum collision theory*. NORTH-HOLLAND PUBLISHING COMPANY, 1975.

[77] F. Salvat, J. D. Martˇnez, R. Mayol, and J. Parellada. Analytical dirac-hartree-fock-slater screening function for atoms (z=1–92). *Phys. Rev. A*, 36:467–474, Jul 1987. doi: 10.1103/PhysRevA.36.467. URL https://link.aps.org/doi/10.1103/PhysRevA.36.467.

[78] Francesc Salvat. Elastic scattering of fast electrons and positrons by atoms. *Phys. Rev. A*, 43:578–581, Jan 1991. doi: 10.1103/PhysRevA.43.578. URL https://link.aps.org/doi/10.1103/PhysRevA.43.578.